Determination of Protein−RNA Interaction Sites in the Cbf5-H/ACA Guide RNA Complex by Mass Spectrometric Protein Footprinting†

Daniel L. Baker,‡ Nicholas T. Seyfried,§ Hong Li,|| Ron Orlando,§ Rebecca M. Terns,*,‡ and Michael P. Terns*,‡

Department of Biochemistry and Molecular Biology, and Genetics, University of Georgia, Athens, Georgia 30602, Complex Carbohydrate Research Center, University of Georgia, Athens, Georgia 30602, and Department of Chemistry and Biochemistry and Institute of Molecular Biophysics, Florida State University, Tallahassee, Florida 32306

Received August 9, 2007; Revised Manuscript Received November 19, 2007

ABSTRACT: Pseudouridylation is one of the most common forms of RNA modification. In eukaryotes and archaea, these modifications are carried out by H/ACA ribonucleoprotein (RNP) complexes, composed of an H/ACA guide RNA and four proteins, including the pseudouridine synthase, Cbf5. Remarkable progress has been made toward understanding the structure and function of H/ACA RNPs, both through mapping of RNA−protein and protein−protein interactions and the availability of X-ray structures, including that of the entire RNP. The pseudouridine synthase, Cbf5, is also the protein that specifically recognizes the guide RNAs. In this work, we have investigated the molecular basis of this key interaction. A mass spectrometric protein footprinting approach was employed to determine the amino acids of archaeal Cbf5 involved in interaction with the guide RNA. We found amino acid protections along the same RNA binding track observed in the crystal structure of the fully assembled complex, indicating that this interaction is established in the subcomplex. However, in addition, we observed a set of protections in the D2 subdomain of Cbf5 that appear to represent a unique, additional interaction of the guide RNA with the protein in the subcomplex. On the basis of these results, we present a model for the Cbf5-guide RNA complex that also incorporates other recent findings. Our analysis suggests that the assembly or function of H/ACA RNPs may be accompanied by dynamic changes in RNA−protein interactions.

One of the most abundant post-transcriptional nucleotide modifications in rRNA is pseudouridylation (*1*). In archaea and eukaryotes, multiple distinct box H/ACA ribonucleoprotein complexes (box H/ACA RNPs, apparently ∼5 in various archaea and ∼100 in humans) are responsible for these modifications (*2*−*5*). These distinct box H/ACA RNPs each contain a different box H/ACA guide RNA, which guides modification via base-pairing with one or more target RNA sites, and a set of four proteins including a conserved pseudouridine synthase, Cbf5 (dyskerin in human, Nap57 in rodents), Gar1, Nop10, and L7Ae (Nhp2 in eukaryotes) (*2*−*5*).

Cbf5 is a member of the TruB family of pseudouridylases, which are all related to the *Escherichia coli* enzyme that modifies tRNAs independent of a guide RNA and accessory proteins (*6*). Cbf5 is the first pseudouridylase found to require other components to function and interact with its substrate (*7*, *8*). The domain structure of Cbf5 is understood from four available Cbf5 crystal structures from three archaeal species, *Pyrococcus furiosus*, *P. abyssi*, and *Archaeoglobus fulgidus*, some with other H/ACA RNP components (*9*−*12*). Cbf5 is composed of two primary domains, the catalytic domain, and a pseudouridine archaeosine tRNA-guanine transgycosylase (PUA) domain composed primarily of the C-terminus (Figure 1A) (*10*, *11*, *13*). Two significant differences have been noted between Cbf5 and TruB: (1) the PUA domain of Cbf5 is larger and includes the N-terminal extension of Cbf5, which envelopes the C-terminus; (2) the thumb-loop, a TruB domain required to stabilize the T-loop of the tRNA substrate, is largely missing in Cbf5 (*10*−*12*). In place of the thumb-loop, Cbf5 contains a $\beta 7/\beta 10$ loop element that is proposed to be important for rRNA substrate interaction (*10*, *12*).

The ability of Cbf5 to interact with guide RNAs does not depend on the other core proteins (*7*, *8*, *14*). Since this finding, an understanding of the amino acids and structures crucial to the independent interaction between Cbf5 and H/ACA RNAs has been sought. The interaction of Cbf5 with the guide RNA in the context of the fully assembled H/ACA RNP was recently illuminated by structure-based models and ultimately a crystal structure of the full complex (*9*, *12*) (Figure 1A). The primary interaction of Cbf5 with the RNA occurs in the PUA domain. The two universally conserved adenines of box ACA (signature sequence element located 3′ of the RNA hairpin and ∼14 nts from the site where the target uridine is positioned (Figure 1B) (*15*, *16*)) are bound in a sequence-specific manner by a number of amino acids within the PUA domain of Cbf5 (*9*). The extensive interaction of the PUA domain with the RNA also encompasses the lower stem of the RNA hairpin.

† This study was supported by NIH Grants RO1 GM54682 (M. T. and R. T.), P41-RR005351 (R. O.), and R01 GM66958-01 (H. L.).

* To whom correspondence should be addressed. E-mail: rterns@bmb.uga.edu, mterns@bmb.uga.edu; phone: (706) 542-1703; fax: (706) 542-1752.

‡ Department of Biochemistry and Molecular Biology, and Genetics, University of Georgia.

§ Complex Carbohydrate Research Center, University of Georgia.

|| Florida State University.

10.1021/bi701606m CCC: $40.75
Published on Web 01/19/2008

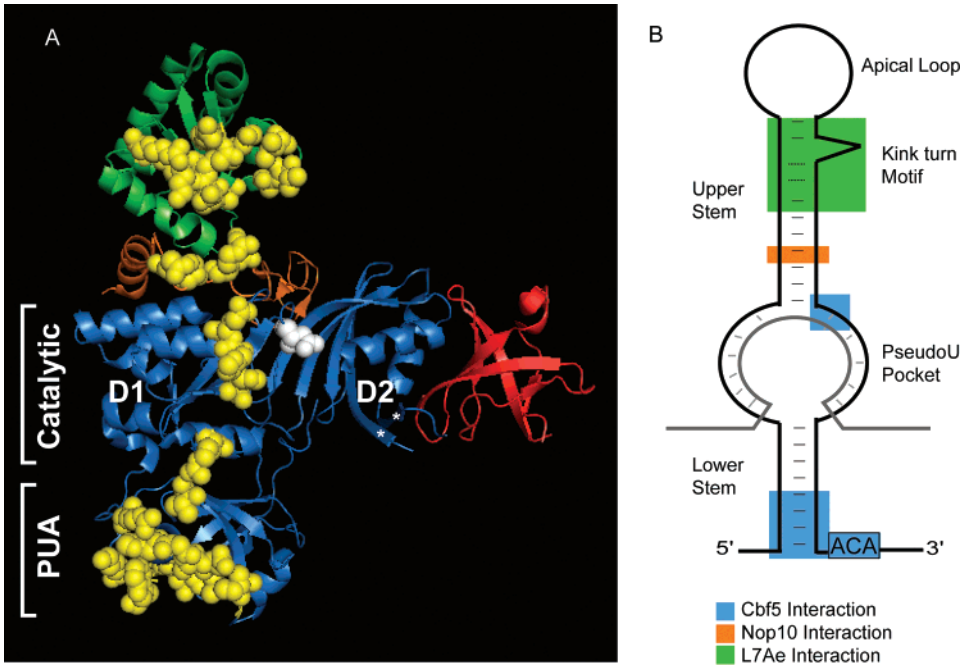

FIGURE 1: RNA binding track in the H/ACA RNP holoenzyme crystal structure. (A) Structures of Cbf5 (blue), Gar1 (red), L7Ae (green), and Nop10 (orange) from the H/ACA RNP crystal structure (2HVY (*9*)). Catalytic and PUA domains, and D1 and D2 subdomains of Cbf5, are indicated. Catalytic Asp 85 is highlighted in white. Amino acids found to interact with the guide RNA are indicated in yellow. β7 and β10 are indicated with asterisks. (B) Diagram of a single-hairpin H/ACA guide RNA with regions of interaction with each protein highlighted.

The other major interaction point of the guide RNA within the H/ACA RNP complex is between the k-turn of the RNA and L7Ae. The k-turn is located in the upper stem (or sometimes in the apical loop) of archaeal H/ACA RNAs (Figure 1B) and is a well-established L7Ae binding site (*7*, *8*, *17*, *18*). Interaction of Nop10 with the upper stem of the RNA also contributes to anchoring the upper region of the RNA to the protein complex. A large number of positively charged residues reside along the guide RNA binding track of the complex, from the PUA domain of Cbf5 to L7Ae.

The target RNA binding site of the guide RNA is loosely positioned over the catalytic cleft of Cbf5 by the interactions observed in the crystal structure (*9*). The target RNA binding site is found in the pseudouridylation pocket, the internal loop that interrupts the basic hairpin structure of the H/ACA RNA and contains the bipartite guide sequence (Figure 1B) (*15*, *16*). The catalytic cleft of Cbf5 is the gap between the two subdomains of the catalytic domain (D1 and D2) that contains the catalytic Asp 85 (Figure 1A). The fourth protein of the complex, Gar1, associates with the D2 subdomain of Cbf5 without contacting the other proteins or the guide RNA (Figure 1A).

While the crystal structure of the full RNP has revealed how the guide RNA interacts with the four-protein complex, analysis and comparison of subcomplexes of the H/ACA RNP are required to understand the contribution of each protein to H/ACA RNP assembly and function. In this study, mutagenesis and a mass spectrometric footprinting method were used to identify specific regions of Cbf5 involved in RNA interactions within the Cbf5-guide RNA subcomplex, which may represent the first complex formed in assembly of the H/ACA RNP (*19*). We adapted a technique that has recently been developed for mapping protein−nucleic acid contact points in which the susceptibility of individual lysines in the protein to modification in the presence and absence of the nucleic acid is monitored by mass spectrometry (*20*−*22*). The approach allowed us to identify specific protections conferred by the RNA at single amino acid resolution. In addition to the sites of interaction observed in the full complex, our results revealed novel interactions that occur in the complex formed by Cbf5 and a guide RNA.

MATERIALS AND METHODS

Mutagenesis and Protein Purification. To generate the Cbf5 mutants, PCR was performed using tagged or untagged Cbf5 constructs in pET21d and pET24d as templates as described previously (*7*) (Table 1 and 2). The genes encoding *P.furiosus* Cbf5, Gar1, Nop10, and L7Ae were obtained as described previously (*7*). The recombinant proteins were expressed in *E. coli* strain BL21+, purified and detected, and the concentration was determined all as described previously (*7*).

In Vitro DNA Synthesis and RNA Transcription. DNA template used for *in vitro* transcription of Pf9, sR29 (similarly sized box C/D RNA), and the target substrate rRNA was generated by PCR or direct annealing of oligonucleotides as described previously (*7*, *23*). The template for the substrate rRNA corresponded to nucleotides 905−917 of *P. furiosus* 16S rRNA with uridines 915−917 replaced by adenines, and flanked by three nucleotide extensions at each end. For large scale transcription of Pf9 and sR29 RNA, PCR product (1000 ng/rxn) was used in a large scale *in vitro* transcription reaction using the Epicentre Ampliscribe T7 Flash Transcription Kit. For small scale transcription of Pf9 RNA and substrate rRNA, annealed oligonucleotides (100 ng) were used as templates for *in vitro* transcription, as described previously (*24*). α^{32}P-GTP was used to uniformly radiolabel guide RNAs, and α^{32}P-UTP was used to label the uridine in the substrate rRNA.

Pseudouridylation Assay. Guide RNA (0.5 pmol) and ^{32}P-labeled rRNA substrate (0.05 pmol) were incubated with

Table 1: Oligonucleotides Used for Generation of Cbf5 Mutants

1. 5′ AAAGCAGGACACGGAGGAACTTTAGCTCCCAAAGTTAGTGGCGTGCTTC C 3′
2. 5′ GGAAGCACGCCACTAACTTTGGGAGCTAAAGTTCCTCCGTGTCCTGCTTT 3′
3. 5′ CTTTAAGAAGGAGATATACCATGGCGCTTCCAGCAGATATAAAAAGAGAAG 3′
4. 5′ CTTCTCTTTTTATATCTGCTGGAAGCGCCATGGTATATCTCCTTCTTAAAG 3′
5. 5′ CCGTTGATGTAGAAAAGGTATTCTAGCCTAGGGATTGGTATCCAAAGTTA TGG 3′
6. 5′ CCATAACTTTGGATACCAATCCCTAGGCTAGAATACCTTTTCTACATCAACGG 3′
7. 5′ CAGAGACCCCCACTTAGAAGCGCTAGACTTAGAACTAGAAAAGTTTACTATATTGAGG 3′
8. 5′ CCTCAATATAGTAAACTTTTCTAGTTCTAAGTCTAGCGCTTCTAAGAGGGGGTCTCTC 3′
9. 5′ CAGAGACCCCCACTTAGAAGCGCTGCGGCCGCAAGACTTAGAACTAGAAAAGTTTACTATATTGAGG 3′
10. 5′ CCTCAATATAGTAAACTTTTCTAGTTCTAAGTCTTGCGGCCGCAGCGCTTCTAAGAGGGGGTCTCTC 3′
11. 5′ CCGTTGATGTAGAAAAGGTATTCATGCCTGCGGATTGGTATCCAAAGTTATGG 3′
12. 5′ CCATAACAATGGATACCAATCGGCAGGCATGAATACCTTTTCTACATCAACG 3′
13. 5′ CACCGGATCCGCGAGAGACGAGGTAAGAAGG 3′
14. 5′ CTTTTCAGCAGCAGCTGGAGGAAATCCCCAATCAGG 3′
15. 5′ TTTCCTCCAGCTGCTGCTGAAAAGGCGGTTGAACACCTACCAAAGG 3′
16. 5′ AAGCTCGAGCGGCCGCTTAGCTTCTATCTCTTTTTTCCCATA 3′

Table 2: Oligonucleotide Combinations Used To Generate Cbf5 Mutants

Cbf5 mutant	oligos
D85A replacement	1 + 2
N-terminal deletion (Δ4−12)	3 + 4
C-terminal deletion (Δ328−343)	5 + 6
VKR deletion (Δ149−151)	7 + 8
VKR (AAA) replacement	9 + 10
R330A	11 + 12
PUA domain (Δ39−246)	first round: 13 + 14; 15 + 16 second round: 13 + 16

purified His-tagged proteins, and the pseudouridylation assay was carried out as described previously (*7*).

Gel Mobility Shift Assays. To determine the effects of mutations on the interaction of Cbf5 with Pf9 H/ACA RNA, approximately equal molar amounts of recombinant wild type and mutant Cbf5 proteins were incubated with the RNA, and gel mobility shift assays were carried out as described previously (*7*). To assess the effect of biotin modification on Cbf5-Pf9 RNA binding by gel shift assay, radiolabeled Pf9 RNA (0.05 pmol) was incubated with unmodified Cbf5 (40 pmol) at a molar ratio of Pf9:Cbf5 = 1:800 in a final volume of 20 μL of 40 mM HEPES−KOH (pH 7.9), 250 mM KCl, and 8 mM $MgCl_2$ for 30 min at 70 °C. The complex was then exposed to sulfosuccinimidyl-6-(biotinamido)hexanoate (EZ-Link Sulfo-NHS-LC-Biotin, Pierce, Rockford, IL, 2 mM) for another 30 min at 70 °C. *E.coli* tRNA (0.25 μg/μL) was then added and incubated for an additional 30 min. In parallel experiments, Cbf5 was modified first with EZ-link Sulfo-NHS-LC-Biotin, half of the sample was taken out and analyzed by SDS-PAGE, and Pf9 RNA and *E.coli* tRNA (0.25 μg/μL) were added to the remaining reaction mix. Reactions were immediately loaded onto nondenaturing 6% polyacrylamide gels containing 0.5× TBE. Electrophoresis was performed at room temperature in 0.5× TBE for 6 h at 115 V. The RNA distribution was visualized by autoradiography after gel drying.

Lysine Modification, in-Gel Trypsin Digestion and MALDI-TOF MS Analysis. Cbf5 was modified with EZ-link Sulfo NHS-LC-biotin in the presence and absence of Pf9 or sR29 RNAs. Typically, Cbf5 (2 μM) was incubated with or without the RNA (150 μM) and modified by the addition of EZ-link Sulfo NHS-biotin (2 μM) under conditions described above. The reactions were quenched by adding lysine (Sigma-Aldrich) in its free amino acid form (10 mM). The samples were then separated via SDS-PAGE, visualized by Coomassie Blue staining, and subjected to in-gel trypsin digestion.

For trypsin digestion, protein bands were excised and sliced into cubes (1 × 1 mm). Gel cubes were dehydrated with 50% (v/v) acetonitrile in 50 mM ammonium bicarbonate for 15 min and subsequently dried under vacuum. The cubes were rehydrated with a solution of sequencing grade trypsin (Promega, 12.5 ng/μL in 50 mM ammonium bicarbonate) and incubated overnight (12−16 h) in a 37 °C water bath. Peptides were extracted from the gel cubes with consecutive washes of 2.5% (v/v) formic acid and 50% (v/v) acetonitrile. Protein digests were analyzed by MALDI-TOF MS using an ABI 4700 Proteomics Analyzer (Applied Biosystems, Foster City, CA). Prior to analysis samples were desalted by ZipTip, mixed 1:1 (v/v) with a saturated solution of α-cyano-4-hydroxycinnamic acid prepared in 50% (v/v) acetonitrile/0.1% (v/v) TFA, and spotted onto the MALDI target. Samples were acquired in the positive ion reflector mode with an acquisition mass range from 700 to 3000 *m*/*z* and a focus at 2000 *m*/*z*. Each spectrum was accumulated for 1000 shots obtained with a laser setting of 4500. External calibration was performed using four standards; des-arg^1-bradykinin (*m*/*z* = 904.468), angiotensin I (*m*/*z* = 1296.685), Glu^1-fibrinopeptide B (*m*/*z* = 1570.678), and neurotensin (*m*/*z* = 1672.92), all monoisotopic masses, respectively.

MS/MS Analysis. In-gel trypsin digests of free and biotin-labeled Cbf5 were analyzed independently on an Agilent 1100 capillary LC (Palo Alto, CA) interfaced directly to a hybrid LTQ-FT linear ion trap/7-Tesla Fourier transform ion cyclotron mass spectrometer (Thermo Electron, San Jose, CA). Mobile phases A and B were H_2O/0.1% (v/v) formic acid and ACN/0.1% (v/v) formic acid, respectively. Each fraction was loaded onto the C18 column (15 cm × 150 μm, Micro-tech Scientific, Vista, CA) at a flow rate of 1 μL/min, and peptides were eluted into the mass spectrometer during a 70 min linear gradient from 5 to 55% (v/v) B. The instrument was set to acquire MS/MS spectra on the nine most abundant precursor ions from each MS scan with a repeat count of 3 and repeat duration of 15 s. Dynamic exclusion was enabled for 160 s. Raw tandem mass spectra were converted into mzXML format and then into a PKL format. The peak lists were then searched using Mascot version 1.9 (Matrix Science, Boston, MA) against the Cbf5

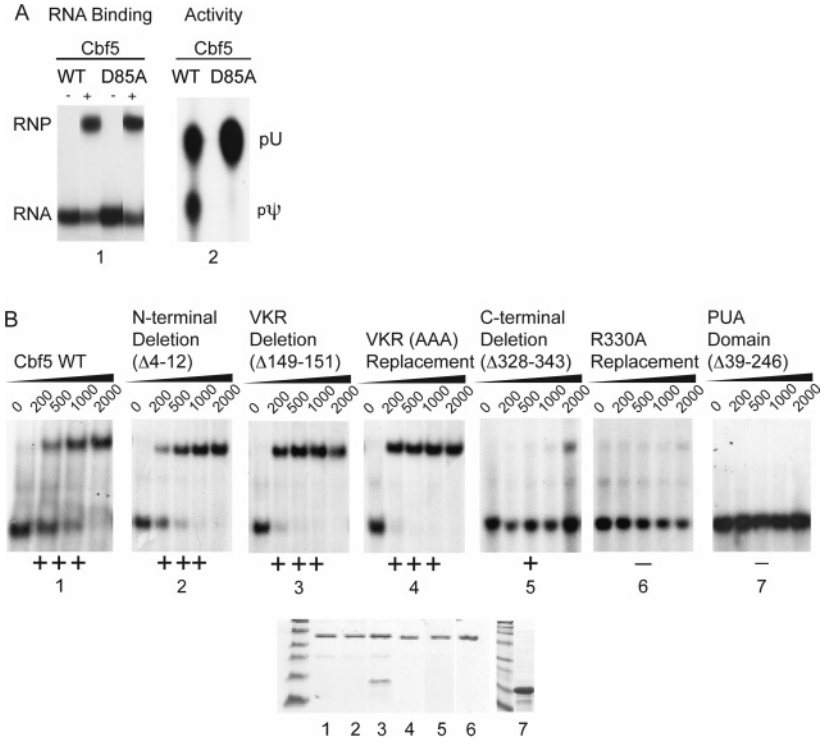

FIGURE 2: Mutational analysis of Cbf5-guide RNA interaction. (A) Effects of mutation of Asp85 on RNA binding and pseudouridylation activity. A purified Cbf5 mutant addressing the proposed catalytic amino acid (D85A) was subjected to a native gel mobility shift assay and *in vitro* pseudouridylation assay to determine the effects this mutation has on Cbf5 and its ability to interact with the guide H/ACA RNA and function (*1*). Purified wild-type Cbf5 and Cbf5 D85A were incubated with radiolabeled Pf9 RNA, and complex formation was assessed analyzed by gel mobility shift analysis and autoradiography (*2*). Pseudouridylation activity of the proteins was assayed as previously described (*7*). Briefly, the purified proteins were incubated with the other three H/ACA RNP proteins, Pf9 RNA, and substrate RNA (containing a single, ^{32}P-labeled target uridine). Pseudouridylation was assessed by TLC separation of uridine (pU) from pseudouridine (pψ) (obtained by nuclease P1 digestion of RNA). (B) RNA binding activity of Cbf5 mutants. Gel mobility shift analysis was performed with the indicated concentrations of Cbf5. An estimate of the extent of the interaction relative to wild-type Cbf5 is provided (+++ to −). SDS-PAGE and Coomassie Blue staining of the protein samples is also shown (1). Wild-type Cbf5 (2). N-terminal deletion (Δ4−12) (3). V149, K150, R151 deletion (4). V149A, K150A, R151A (5). C-terminal deletion (Δ328−343) (6). R330A replacement (7). PUA domain (Δ39−246).

amino acid sequence (PF1785). Searches were performed against the Cbf5 sequence using the following parameters: trypsin enzyme specificity, five missed cleavages, a variable LC-biotin modification on Lys of (+339.16 Da), a peptide tolerance of 50 parts-per-million, and a fragment ion tolerance of 0.6 Da.

Data Interpretation. Protection events were qualitatively assigned as the appearance of a peak corresponding to a single LC-biotin-modified lysine within a peptide (+339.2 Da) in the modified protein spectrum and the absence or reduction of the modification peak in the modified ribonucleoprotein complex from MALDI-TOF spectra (*21*, *22*). The protection was considered to be significant when the average intensity of a modifiable peak was reduced by more than 85% in the ribonucleoprotein complex, as was established in previous studies (*21*, *22*). To accurately identify the protection events, a reference peak (m/z = 1482.91, AA: 157−168, seq:VYYIEVLEIEGR) not affected by biotinylation (no lysines), was used to normalize peak intensities between samples. Data were compiled for each peptide fragment and analyzed from two to six independent experiments.

RESULTS

PUA Domain Mutations Affect Interaction of Cbf5 with the H/ACA Guide RNA. Cbf5 is the H/ACA RNP protein that specifically recognizes guide RNAs and secures the lower half of the RNAs in a position that places the target uridine (of the subsequently bound substrate RNA) near its own catalytic center. In this work we have focused on the molecular basis of the key interaction between these components. Gel shift assays of mutant proteins can provide an indication of the involvement of amino acids or regions of a protein in an RNA−protein interaction in solution. Here, we tested the ability of a collection of Cbf5 mutants to interact with an H/ACA guide RNA in the absence of the other H/ACA RNP proteins.

The universally conserved amino acid D85 is required for function (*25*) and is thought to play a direct role in catalysis of substrate modification. We replaced this amino acid with alanine (D85A) to determine its effect on interaction with Pf9 RNA. The replacement mutation completely abolished pseudouridylation but did not have an effect on the Cbf5-Pf9 RNA interaction, consistent with the specific proposed role of this amino acid in catalysis (Figure 2A).

The N-terminus of Cbf5 wraps around the PUA domain and is not present in the guide RNA-independent bacterial TruB enzymes. Truncation of 42 amino acids from the N-terminus of Cbf5 (Δ4−45) resulted in insoluble protein, but a shorter truncation (Δ4−12) was soluble and interacted with Pf9 RNA to a similar extent as wild-type (Figure 2B, panel 2), indicating that these amino acids are not important in guide RNA binding.

Another region of interest in Cbf5 is the $\beta 7/\beta 10$ hairpin loop, which is located in the catalytic domain and thought to function analogously to the thumb-loop domain of TruB (*10*, *12*). The TruB thumb-loop domain is disordered in the absence of substrate RNA but becomes ordered and clamps down on the target tRNA upon interaction (*13*). We both replaced and deleted three highly conserved (and mostly positively charged) amino acids within the $\beta 7/\beta 10$ hairpin loop region (V149A, K150A, and R151A) to determine their involvement in the interaction between Cbf5 and Pf9 RNA (Figure 2B, panels 3, 4). In both cases, no negative impact (and in fact a slight increase) in guide RNA binding relative to wild-type was observed. These results suggest that if the $\beta 7/\beta 10$ hairpin loop of Cbf5 plays a role in RNA binding within the H/ACA RNP, the interaction likely involves the substrate RNA.

The C-terminus of Cbf5 forms the PUA domain, and a number of amino acids in this domain were observed to interact with the H/ACA guide RNA in the full complex crystal structure (*9*). We found that truncation of the last 16 amino acids of Cbf5 had a strong negative effect on guide RNA binding in gel shift assays (Figure 2B, panel 5). Moreover, replacement of the conserved amino acid R330 with an alanine also disrupted binding (Figure 2, panel 6), indicating that this amino acid is important in guide RNA interaction in solution. In the full complex crystal structure, this amino acid was observed to interact with the RNA (*9*).

To test whether the PUA domain alone was capable of sufficiently stable interaction with the guide RNA to be detected in gel shift assays, we constructed a PUA domain by connecting the N-terminus of Cbf5 with the C-terminal domain via a three-alanine linker ($\Delta 39-246$). This protein was highly soluble but did not interact with the guide RNA (Figure 2B, panel 7), suggesting that interactions with other regions of Cbf5 also contribute significantly to formation of the Cbf5-guide RNA complex.

Mass Spectrometric Footprinting Approach To Map Cbf5-H/ACA Guide RNA Interactions. Analysis of crystal structures revealed a concentration of surface-exposed positive residues along the proposed catalytic cleft of Cbf5 and extending down into the PUA domain and upward into Nop10 and L7Ae, creating a favorable RNA-binding platform (*10*−*12*). Mutational analysis provides further evidence for the importance of conserved basic residues in guide RNA binding (Figure 2B and (*10*)). In Cbf5, the most prevalent positively charged amino acid is lysine, which accounts for 29 of the 343 total amino acids. Taking advantage of the large number of lysines, we adapted a recently established mass spectrometry (MS)-based footprinting technique, which had previously been employed to map contact points between proteins and DNA (*20*−*22*). The protein footprinting method detects the protection of solvent-accessible lysines from biotinylation upon nucleic acid binding.

For these experiments, we first established conditions where the biotinylation of the surface lysines in Cbf5 was efficient but would not disrupt a pre-existing Cbf5-guide RNA complex. Using gel mobility shift assays, we found that prior biotinylation of Cbf5 with 2 μM biotin prevented subsequent complex formation upon addition of the guide RNA (Figure 3A), indicating that lysines of interest (important for the interaction) were being efficiently modified under these reaction conditions. However, at the same time, the majority of preformed Cbf5-guide RNA complexes were not disrupted by biotinylation with 2 μM biotin (Figure 3B), indicating that the lysines needed for a stable interaction are effectively shielded from modification in the ribonucleoprotein complex. We proceeded with footprinting using these conditions, which had proven to provide for efficient modification of relevant lysines when exposed (Figure 3A), without vast disruption of the preformed complex (Figure 3B).

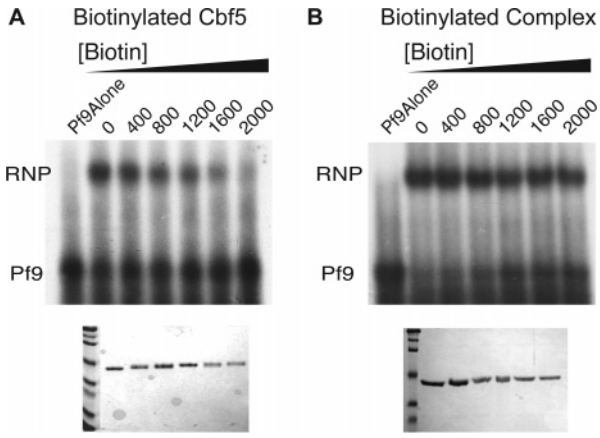

FIGURE 3: Effect of increasing biotinylation levels on Cbf5-guide RNA complexes. (A) Effect of biotinylation of Cbf5 on subsequent complex formation. Cbf5 was biotinylated with indicated concentrations of Sulfo NHS-Biotin and then incubated with Pf9 RNA. Complex formation was examined by gel mobility shift analysis. (B) Effect of biotinylation on existing Cbf5-guide RNA complexes. Preformed Cbf5-Pf9 complexes were biotinylated with indicated concentrations of sulfo NHS-biotin and then examined by gel mobility shift analysis. Lower panels show SDS-PAGE and Coomassie Blue staining of the protein samples.

Points of interaction between Cbf5 and the guide RNA were determined by comparison of three samples: unmodified Cbf5, biotinylated Cbf5, and biotinylated Cbf5 in the presence of RNA. Again, Pf9 was the H/ACA RNA used to assess the interaction with Cbf5. sR29, a box C/D RNA of similar size, was used as a control. sR29 fails to interact with Cbf5 in gel mobility shift assays (*7*), though nonspecific interaction with this RNA could occur in the footprinting assays, which lack competitor RNA. We optimized the concentration of RNA in our biotinylation assays to minimize "nonspecific" protections (defined with sR29) while maintaining detectable protection with Pf9.

After biotinylation, the samples were subjected to SDS-PAGE prior to trypsin proteolysis to separate the RNA from the protein and to denature Cbf5. This provided for reproducible hydrolysis with trypsin. After in-gel trypsin digestion, the three samples were analyzed by MALDI-TOF MS for the initial identification of peptide fragments. The monoisotopic masses of peptides containing a modified lysine are increased by 339.2 Da (Figure 4A). The biotinylated peptides also lose a cleavage site because trypsin does not cleave at the modified lysines.

MALDI-TOF MS not only allowed for the identification of lysine residues that were readily biotinylated in the free protein sample but also for determination of whether those lysines were protected from biotinylation in the ribonucleoprotein samples. A lysine was considered protected if the peak intensity of the corresponding biotinylated peptide fragment was reduced by at least 85% from the modified

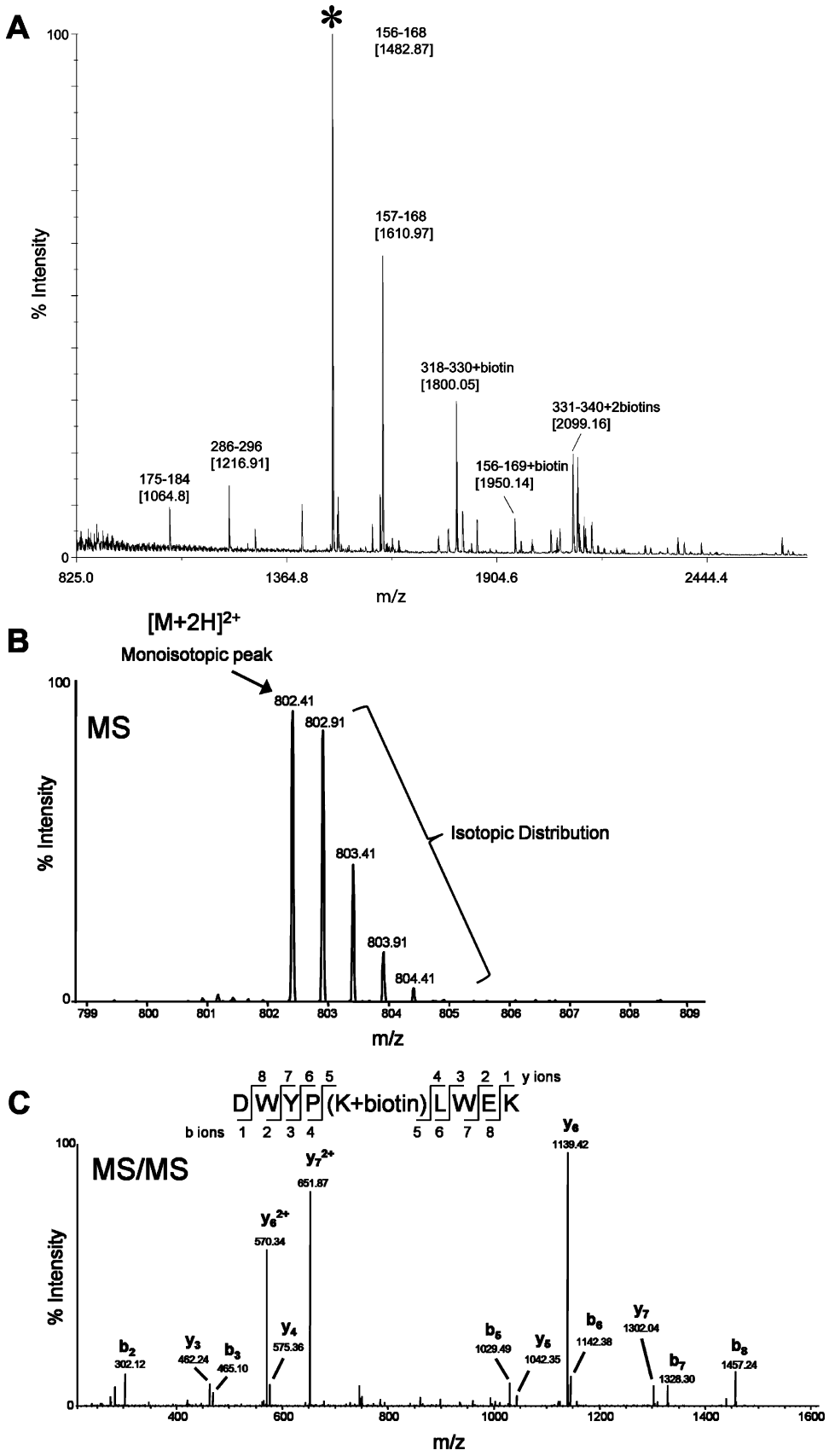

FIGURE 4: Analysis of Cbf5 biotinylation by mass spectrometry. (A) A typical MALDI-TOF spectrum of trypsin-digested biotinylated Cbf5. Isotopic resolution of all of the peptide peaks was obtained, allowing assignment of singly charged unmodified and biotinylated peptide fragments. The reference peak (1482.87) used to normalize between spectra is indicated with an asterisk. (B) A typical LTQ-FT survey scan of a doubly charged biotinylated peptide fragment (monoisotopic $m/z = 802.41$) showing the isotopic distribution. The m/z value of this ion corresponds to peptide fragment 331−339 + 1 biotin. (C) MS/MS analysis of the ion at $m/z = 802.41$, shown in B, confirms the peptide fragment identity and that this fragment was biotinylated at Lys 335. The *y* ion series were derived from internal fragmentation of the peptide bonds, providing a sequence read from the C-terminus to the N-terminus.

Table 3: Lysine Biotinylation Protection Results

no RNA			Pf9 RNA		sR29 RNA	
$[M + H]^+$	fragment	biotinylated lysine	protection	%	protection	%
1263.00	12−19	18	no	65 ± 7	no	43 ± 9
2924.82	19−41	24	no	79 ± 13	no	82 ± 10
2468.30	71−87	77	yes	96 ± 8	no	55 ± 14
3051.98	78−101	87	yes	100 ± 0	no	71 ± 9
1779.22	88−101	98	yes	88 ± 9	no	69 ± 16
3169.97	102−127	111	yes	100 ± 0	no	64 ± 16
2903.50	112−133	127	no	23 ± 24	N/A	N/A
2634.50	128−146	133	no	66 ± 17	no	67 ± 14
1950.25	157−169	157	yes	86 ± 10	no	53 ± 6
2727.50	256−279	259	yes	97 ± 7	yes	100 ± 0
2820.00	260−285	279	no	33 ± 33	no	61 ± 12
2462.00	297−315	304	no	58 ± 6	N/A	N/A
1398.86	316−325	317	yes	100 ± 0	N/A	N/A
1800.17	318−330	325	yes	93 ± 5	no	56 ± 20
1604.02	331−339	335	yes	94 ± 7	no	63 ± 24

protein alone sample to the modified ribonucleoprotein sample (*21*, *22*).

Another portion of each sample was then analyzed using Fourier-transform mass spectrometry (Figure 4B), which provided the ability to subject selected ions to tandem MS (MS/MS) at high resolution and mass accuracy. The unique MS/MS spectrum associated with each fragment was matched to the Cbf5 sequence using a Mascot database searching algorithm (*26*). These were used to confirm the identities of each peptide fragment and the presence of lysine biotinylation on Cbf5 (Figures 4B and 4C).

Protection of Cbf5 by an H/ACA Guide RNA. In the absence of RNAs, we consistently observed modification of 15 of the 29 lysines in Cbf5 (Table 3, biotinylated lysine). Some lysines were likely not detected due to the inability of MS to detect peptide fragments below a certain size.

The patterns of lysine protection (greater than 85% reduction in biotinylation in the presence of RNA) observed in multiple experiments were generally consistent. Typical instances of protection and lack of protection can be seen in Figure 5. In Figure 5B, the indicated peak ($[M + H]^+ = 2904.70$) is produced by fragment 112−133 with a biotinylated lysine at position 127 (confirmed by MS/MS analysis). Addition of the H/ACA RNA produces little to no shielding at this site (Figure 5C), indicating that Pf9 RNA does not interact with this region of the protein. Biotinylation of Cbf5 also produces a peak ($[M + H]^+ = 1604.02$) corresponding to peptide fragment 331−339 with a biotinylated lysine at position 335 (confirmed by MS/MS analysis) (Figure 5E). However, this peak is lost upon addition of Pf9 (Figure 5F), indicating that this lysine is protected by Pf9.

Of the 15 biotinylated lysines in Cbf5, nine were found to be protected by Pf9 RNA (Table 3). The protected lysines were Lys 77, Lys 87, Lys 98, Lys 111, Lys 157, Lys 259, Lys 317, Lys 325 and Lys 335. Only one of these lysines (Lys 259) was also protected by sR29. We did not observe any unique protections for sR29.

DISCUSSION

The focus of this work has been to understand how Cbf5, the catalytic component of H/ACA RNPs, independently recognizes and interacts with the box H/ACA guide RNA. Evidence suggests that binding of the guide RNA by Cbf5 may be the first step in assembly of the H/ACA RNP in eukaryotes (*19*). We used traditional mutagenesis and a relatively new lysine protection approach to biochemically map recognition points between Cbf5 and a box H/ACA RNA in solution. Our results indicate that the major regions of interaction seen in the fully assembled, four-protein enzyme are established in the Cbf5-guide RNA complex (detailed below). However, we have found that in the absence of the other proteins (which contribute substantial guide RNA interactions in the final complex, see Figure 1), additional interactions occur between Cbf5 and the guide RNA.

To illustrate the results of our studies, we have highlighted the amino acids identified in our analysis of the Cbf5-guide RNA subcomplex in the context of the structure of the full complex (Figure 6A, red and orange) (*9*). In addition, we have highlighted the amino acids in Cbf5 (and L7Ae and Nop10) that are apparently protected by the guide RNA in the full complex (Figure 6A, yellow and orange). We calculated the apparent protection of each amino acid observed in the RNA−protein cocrystal structure (relative to the same structure lacking the RNA) as the change in its solvent-accessible surface area (*27*) in the presence and absence of the RNA. The amino acids implicated in the RNA binding sites in both the Cbf5-guide RNA subcomplex (this study) and the full H/ACA RNP (crystal structure (*9*)) are shown in orange in Figure 6A, and those unique to the Cbf5-guide RNA complex are shown in red. For direct comparison of the RNA protections observed in the two complexes, Table 4 shows all of the lysines present in Cbf5 and their observed protections in the full complex and Cbf5-guide RNA complex.

Most of the amino acids implicated in RNA interaction in our work fall along the linear RNA binding pathway observed in the full complex crystal structure (*9*) (Figure 6A, Table 4). (Because our analysis and the full complex crystal structure both use proteins from *P. furiosus*, all references to specific amino acids correlate directly.) The pathway is established by interactions between box ACA and the lower stem of the RNA, and the PUA domain of Cbf5, and extended by interactions between the base of the upper stem of the RNA and the catalytic domain of Cbf5 (see also Figure 1). In the full complex, extensive interactions with L7Ae anchor the upper region of the RNA. In the Cbf5-guide RNA subcomplex, our findings suggest that the upper

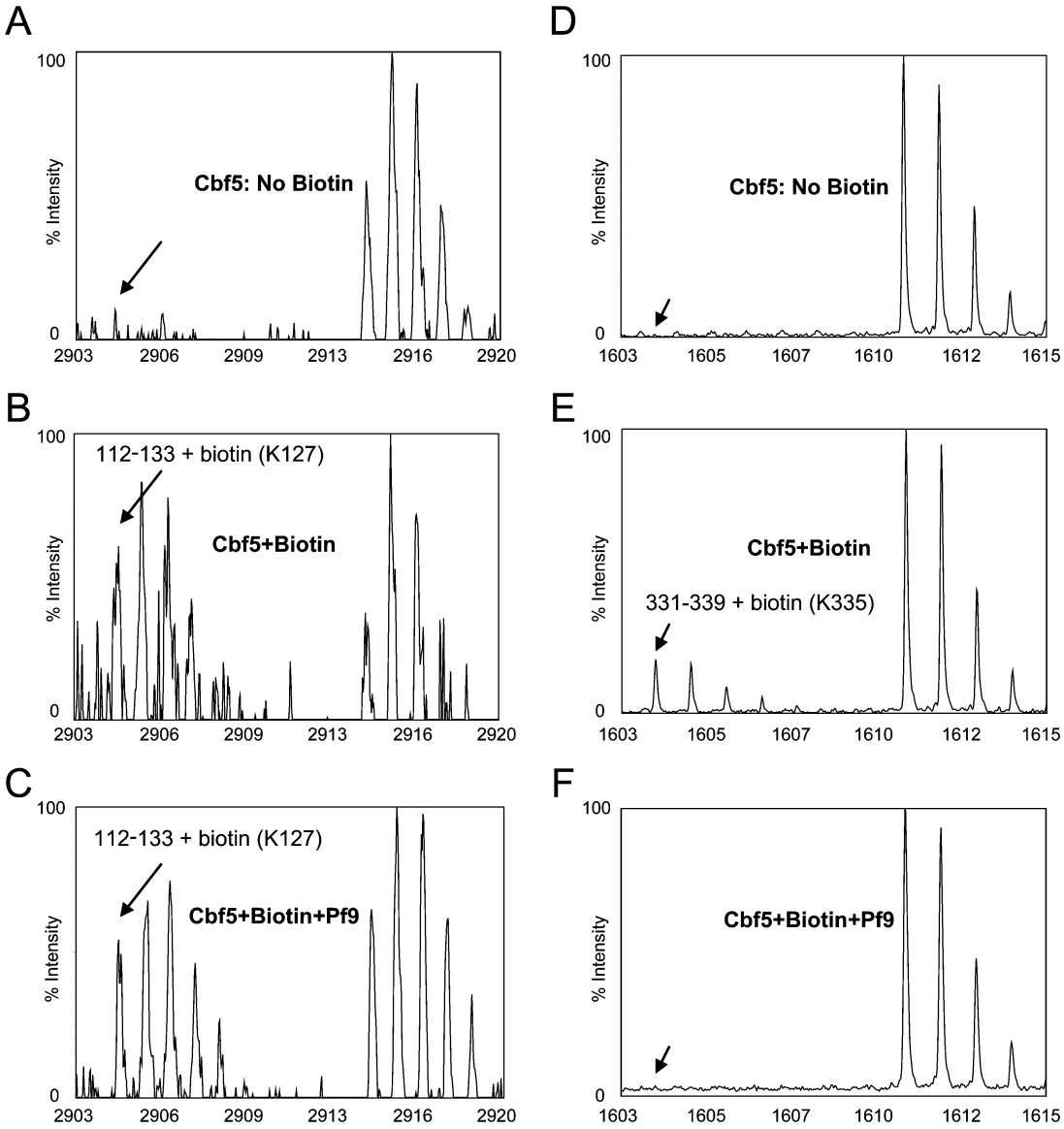

FIGURE 5: MALDI-TOF identification of Cbf5 lysine residues protected from modification by guide RNA. (A−C) The isotopic distribution of the ion (monoisotopic $m/z = 2904.70$) that corresponds to the biotinylated peptide fragment 112−133 (Lys 127) is shown as an example of a fragment not protected by the RNA. The ion arises upon biotinylation of Cbf5 (B) and is retained in the biotinylated RNA−protein complex sample (C). (D−F) The isotopic distribution of the ion (monoisotopic $m/z = 1604.02$) that corresponds to peptide fragment 331−339 (Lys 335) is shown as an example of protection. The peak is observed in the modified Cbf5 sample (E) but not in the presence of Pf9 RNA (F).

region of the RNA interacts with a newly identified site in Cbf5.

The Common RNA Binding Path in the Cbf5-Guide RNA and Fully Assembled Complexes. The PUA domain of Cbf5 serves a critical role in the recognition and binding of the H/ACA RNA. Previously, the Branlant laboratory showed that a Cbf5 mutant lacking the PUA domain was incapable of interacting with H/ACA RNAs (*8*). From the crystal structure of the full complex, it is clear that the primary recognition of the H/ACA RNA occurs via numerous RNA−protein contacts within the PUA domain (*9*) (Figure 6A). Our results indicate that the interaction of the PUA domain of Cbf5 with the guide RNA is the same in the full complex and the Cbf5-guide RNA subcomplex.

The element common to H/ACA RNAs, box ACA, is bound in a sequence-specific manner by interactions with multiple amino acids in the PUA domain of Cbf5 (*9*). Only one lysine, Lys 259, interacts directly with box ACA in the full complex. We found that this lysine is protected from biotinylation in the Cbf5-guide RNA complex as well as from solvent in the full complex (Figure 6A, Table 4). Lys 259 was the only lysine also protected by sR29 in our experiments. This lysine hydrogen bonds with the terminal phosphate group of the guide RNA in the crystal structure, and though we optimized conditions to minimize nonspecific interaction, it is possible that regions of the protein involved in guide RNA binding could interact with the control RNA. Lys 317 is found adjacent to Gly 318, which hydrogen bonds with the central cytosine of box ACA, and is protected from solvent by the guide RNA in the full complex (Table 4). This amino acid is also protected by the RNA in the Cbf5-guide RNA complex (Figure 6A, Table 4).

Beyond box ACA, the lower stem of the guide RNA makes a series of interactions along a path made up primarily of positively charged residues in the PUA domain of Cbf5 (*9*) (Figure 6A). We found that mutation of Arg 330, which

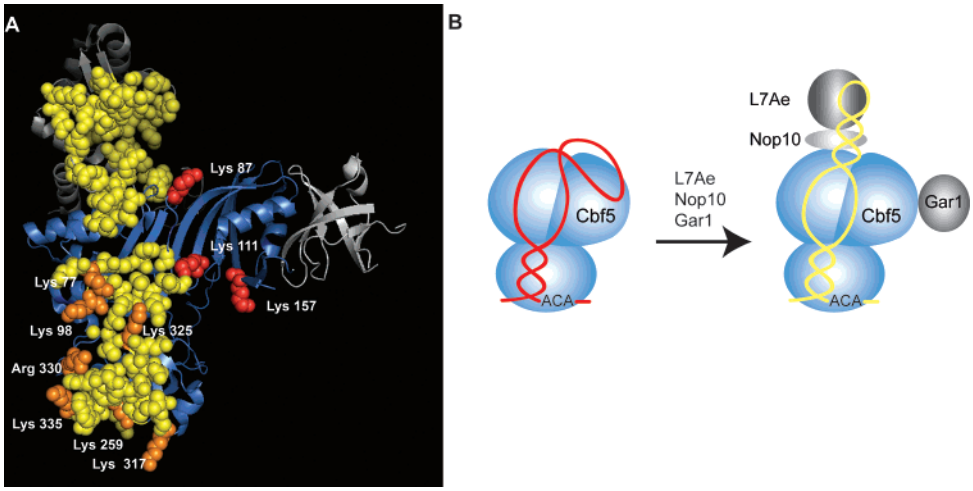

FIGURE 6: Comparison of guide RNA interactions in the Cbf5-guide RNA complex and fully assembled H/ACA RNP complex. (A) Cbf5 is shown in blue, and the other proteins in shades of gray. Sites protected by the guide RNA in the full complex crystal structure are indicated in yellow (Table 4, 2HVY, ref *9*). Amino acids implicated in RNA interaction in the Cbf5-guide RNA complex in this work are shown in red. Amino acids identified in both studies are orange. (B) Emerging model of changes in guide RNA−protein interactions in subcomplexes of the H/ACA RNP. Interactions of lower regions of the guide RNA with Cbf5 are established in the Cbf5-guide RNA complex. Nucleotides that will form the k-turn and apical loop of the guide RNA interact with the catalytic domain of Cbf5 in this complex. L7Ae effectively competes for binding in upper regions of the guide RNA and induces formation of the k-turn and upper stem (and thus also the pseudouridylation pocket) of the guide RNA (*28*).

Table 4: Comparison of Lysine Protection in the Full H/ACA RNP and Cbf5-Guide RNA Complexes

Cbf5 domain	lysine	full complex (computed protection (Å^2))[a]	Cbf5-guide RNAcomplex (footprinting)[b]	location
PUA	18	0.0	no	off track
	24	0.0	no	off track
	279	0.0	no	off track
	304	0.0	no	off track
	259	2.8	yes	common track
	317	2.4	yes	common track
	325	0.2	yes	common track
	335	3.8	yes	common track
Catalytic	77	2.9	yes	common track
	98	1.5	yes	common track
	127	0.0	no	off track
	133	0.0	no	off track
	87	0.0	yes	proposed new site
	111	0.0	yes	proposed new site
	157	0.0	yes	proposed new site

[a] Lysine protection in the full complex (PDB code 2HVY) was estimated as the difference in the solvent accessible area (Å^2) of the lysine in the presence and absence of the guide RNA. Solvent accessible area was computed using the CNS program with a probe radius of 1.4 Å (*27*). The greater the difference, the more protection of the lysine by the guide RNA is observed in the crystal structure. A value of zero indicates no protection. [b] Lysine protection from biotinylation provided by Pf9 RNA (see Table 3).

interacts directly with the lower stem in the crystal structure (*9*), nearly eliminates interaction between Cbf5 and the guide RNA in the subcomplex (Figure 2B, panel 6, and Figure 6A). In addition, in our footprinting experiments we observed protection of the two lysines found along the lower stem binding path in the PUA domain. Lys 335, which directly contacts the phosphate backbone of the lower stem of the RNA in the full complex crystal structure (*9*), is protected in the Cbf5-guide RNA complex (Figure 6A, Table 4). Furthermore, Lys 325, which is also shielded from solvent by the RNA in the full complex (Table 4) and is adjacent to Val 326, which directly interacts with the lower stem of the RNA (*9*), is protected in the subcomplex.

At the same time, the four biotinylated lysines present in the PUA domain outside the RNA binding track (Lys 18, Lys 24, Lys 279, and Lys 304) were not protected in the Cbf5-guide RNA complex (Table 4). Finally, truncation of a portion of the N-terminus (Δ4−13) of the PUA domain had little to no effect on binding in the subcomplex (Figure 2B). These results indicate that these regions of the PUA domain are also not involved in RNA interaction in the Cbf5-guide RNA subcomplex.

Within the catalytic domain, we observed two more protections that lie along the established RNA binding track. Lys 77 and Lys 98 are both located in the D1 subdomain in close proximity to the H/ACA RNA in the full complex, and though no molecular interactions with these amino acids were reported in the crystal structure, both are protected from solvent by the RNA (*9*). On the other hand, two biotinylatable lysines in the D2 subdomain of Cbf5, Lys 127 and Lys 133, were not protected in our experiments (Table 4).

In summary, all of the lysines that are protected from solvent by the RNA in the crystal structure of the full complex are also protected from biotinylation in the Cbf5-guide RNA complex (Table 4). In addition, all of the lysines that we found are not protected by the RNA in the Cbf5-guide RNA complex are also not protected by the RNA in the full complex. These results strongly suggest that the interactions of the guide RNA with Cbf5 found in the fully assembled complex are also present in the Cbf5-guide RNA complex. In addition, however, we found that a cluster of lysines in the D2 subdomain of Cbf5 is protected in the Cbf5-guide RNA complex but not in the full complex (see below).

Evidence of Additional Interactions in the Cbf5-Guide RNA Complex. Our results appear to establish a common RNA binding track in the full complex and Cbf5-guide RNA

subcomplex that is primarily founded on interactions with the PUA domain. In the fully assembled complex, the other great density of interactions occurs between the k-turn of the RNA and L7Ae at the top of the complex. While the PUA domain of Cbf5 undoubtedly contributes both specificity and strength to the interaction with the H/ACA guide RNA, it is not sufficient for interaction with the RNA (Figure 2B, panel 7, and ref *8*). It is clear that regions within the catalytic domain make significant contributions to RNA binding in the Cbf5-guide RNA subcomplex. Our results indicate that in the absence of the other proteins, additional interactions occur between the catalytic domain of Cbf5 and the guide RNA.

We found evidence of three additional lysine protections in the catalytic domain of Cbf5 in the subcomplex: Lys 87, Lys 111, and Lys 157 (Table 4). These protections are on the front face of the D2 subdomain of Cbf5 (Figure 6A, red), outside the RNA binding path in the full complex, which lies along the front face of the D1 subdomain (Figure 6A, yellow and orange). There is no evidence for interaction of this region of the protein with the RNA in the full complex. We propose that these protections reflect a unique interaction of the guide RNA with Cbf5 in the Cbf5-guide RNA complex.

Model of the Cbf5-Guide RNA Complex and Role of L7Ae in Guide RNA Positioning. On the basis of the results of this study and other recent work, we propose a specific model for the organization of the Cbf5-guide RNA complex and its relationship to the fully assembled complex (Figure 6B). We recently determined the nucleotides of the Pf9 guide RNA that interact with Cbf5 in the Cbf5-guide RNA complex in nucleotide protection assays (*28*). These studies revealed expected protections at box ACA, the lower stem, and pseudouridylation pocket (see Figure 1B) but also convincing unexpected protection of the 5′ half of the k-turn and apical loop of the RNA. Taken together, the results of the two studies strongly suggest a novel interaction between the 5′ strand of the k-turn and apical loop of the guide RNA, and the D2 subdomain of Cbf5 in the subcomplex. The importance of this interaction in the stability of the Cbf5-guide RNA complex is demonstrated by the disruption of the complex that occurs upon mutation of this region of the RNA (*7*).

While it is clear that Cbf5 is the H/ACA RNP protein that specifically recognizes H/ACA guide RNAs, the intermediates that may be involved in the assembly and function of the H/ACA RNP have not yet been fully defined, and that work may provide additional insight on the importance of the novel interaction that occurs in the subcomplex. Two of the lysines identified as part of the novel interaction site (Lys 87 and Lys 111) are highly conserved and present in the human protein. Interestingly, we have also found that *in vitro* the addition of L7Ae (which interacts with the 5′ half of the k-turn in the fully assembled enzyme, see Figure 1) to the Cbf5-guide RNA complex eliminates the protection of this region of the RNA by Cbf5 (*28*). The findings indicate that L7Ae successfully competes with the novel interaction site on Cbf5 for binding to the upper region of the guide RNA, repositions the guide RNA, and also provides needed strength in binding the guide RNA in the pseudouridylation guide complex.

REFERENCES

1. Maden, B. E. (1990) The numerous modified nucleotides in eukaryotic ribosomal RNA, *Prog. Nucleic Acid Res. Mol. Biol. 39*, 241−303.
2. Matera, A. G., Terns, R. M., and Terns, M. P. (2007) Non-coding RNAs: lessons from the small nuclear and small nucleolar RNAs, *Nat. Rev. Mol. Cell Biol. 8*, 209−220.
3. Kiss, T., Fayet, E., Jady, B. E., Richard, P., and Weber, M. (2006) Biogenesis and intranuclear trafficking of human box C/D and H/ACA RNPs, *Cold Spring Harbor Symp. Quant. Biol. 71*, 407−417.
4. Reichow, S. L., Hamma, T., Ferre-D'Amare, A. R., and Varani, G. (2007) The structure and function of small nucleolar ribonucleoproteins, *Nucleic Acids Res. 35* (5), 1452−1464.
5. Terns, M., and Terns, R. (2006) Noncoding RNAs of the H/ACA family, *Cold Spring Harbor Symp. Quant. Biol. 71*, 395−405.
6. Koonin, E. V. (1996) Pseudouridine synthases: four families of enzymes containing a putative uridine-binding motif also conserved in dUTPases and dCTP deaminases, *Nucleic Acids Res. 24*, 2411−2415.
7. Baker, D. L., Youssef, O. A., Chastkofsky, M. I., Dy, D. A., Terns, R. M., and Terns, M. P. (2005) RNA-guided RNA modification: functional organization of the archaeal H/ACA RNP, *Genes Dev. 19*, 1238−1248.
8. Charpentier, B., Muller, S., and Branlant, C. (2005) Reconstitution of archaeal H/ACA small ribonucleoprotein complexes active in pseudouridylation, *Nucleic Acids Res. 33*, 3133−3144.
9. Li, L., and Ye, K. (2006) Crystal structure of an H/ACA box ribonucleoprotein particle, *Nature 443*, 302−307.
10. Hamma, T., Reichow, S. L., Varani, G., and Ferre-D'Amare, A. R. (2005) The Cbf5-Nop10 complex is a molecular bracket that organizes box H/ACA RNPs, *Nat. Struct. Mol. Biol. 12*, 1101−1107.
11. Manival, X., Charron, C., Fourmann, J. B., Godard, F., Charpentier, B., and Branlant, C. (2006) Crystal structure determination and site-directed mutagenesis of the Pyrococcus abyssi aCBF5-aNOP10 complex reveal crucial roles of the C-terminal domains of both proteins in H/ACA sRNP activity, *Nucleic Acids Res. 34*, 826−839.
12. Rashid, R., Liang, B., Baker, D. L., Youssef, O. A., He, Y., Phipps, K., Terns, R. M., Terns, M. P., and Li, H. (2006) Crystal structure of a Cbf5-Nop10-Gar1 complex and implications in RNA-guided pseudouridylation and dyskeratosis congenita, *Mol. Cell 21*, 249−260.
13. Hoang, C., and Ferre-D'Amare, A. R. (2001) Cocrystal structure of a tRNA Psi55 pseudouridine synthase: nucleotide flipping by an RNA-modifying enzyme, *Cell 107*, 929−939.
14. Normand, C., Capeyrou, R., Quevillon-Cheruel, S., Mougin, A., Henry, Y., and Caizergues-Ferrer, M. (2006) Analysis of the binding of the N-terminal conserved domain of yeast Cbf5p to a box H/ACA snoRNA, *RNA 12*, 1868−1882.
15. Ni, J., Tien, A. L., and Fournier, M. J. (1997) Small nucleolar RNAs direct site-specific synthesis of pseudouridine in ribosomal RNA, *Cell 89*, 565−573.
16. Ganot, P., Caizergues-Ferrer, M., and Kiss, T. (1997) The family of box ACA small nucleolar RNAs is defined by an evolutionarily conserved secondary structure and ubiquitous sequence elements essential for RNA accumulation, *Genes Dev. 11*, 941−956.
17. Rozhdestvensky, T. S., Tang, T. H., Tchirkova, I. V., Brosius, J., Bachellerie, J. P., and Huttenhofer, A. (2003) Binding of L7Ae protein to the K-turn of archaeal snoRNAs: a shared RNA binding motif for C/D and H/ACA box snoRNAs in Archaea, *Nucleic Acids Res. 31*, 869−877.
18. Moore, T., Zhang, Y., Fenley, M. O., and Li, H. (2004) Molecular basis of box C/D RNA-protein interactions; cocrystal structure of archaeal L7Ae and a box C/D RNA, *Structure (Camb.) 12*, 807−818.
19. Yang, P. K., Hoareau, C., Froment, C., Monsarrat, B., Henry, Y., and Chanfreau, G. (2005) Cotranscriptional recruitment of the pseudouridylsynthetase Cbf5p and of the RNA binding protein Naf1p during H/ACA snoRNP assembly, *Mol. Cell. Biol. 25*, 3295−3304.
20. Kvaratskhelia, M., Miller, J. T., Budihas, S. R., Pannell, L. K., and Le Grice, S. F. (2002) Identification of specific HIV-1 reverse transcriptase contacts to the viral RNA:tRNA complex by mass spectrometry and a primary amine selective reagent, *Proc. Natl. Acad. Sci. U.S.A. 99*, 15988−15993.

21. Shell, S. M., Hess, S., Kvaratskhelia, M., and Zou, Y. (2005) Mass spectrometric identification of lysines involved in the interaction of human replication protein a with single-stranded DNA, *Biochemistry 44*, 971−978.
22. Shkriabai, N., Patil, S. S., Hess, S., Budihas, S. R., Craigie, R., Burke, T. R., Jr., Le, Grice, S. F., and Kvaratskhelia, M. (2004) Identification of an inhibitor-binding site to HIV-1 integrase with affinity acetylation and mass spectrometry, *Proc. Natl. Acad. Sci. U.S.A. 101*, 6894−6899.
23. Speckmann, W. A., Li, Z. H., Lowe, T. M., Eddy, S. R., Terns, R. M., and Terns, M. P. (2002) Archaeal guide RNAs function in rRNA modification in the eukaryotic nucleus, *Curr. Biol. 12*, 199−203.
24. Narayanan, A., Lukowiak, A., Jady, B. E., Dragon, F., Kiss, T., Terns, R. M., and Terns, M. P. (1999) Nucleolar localization signals of box H/ACA small nucleolar RNAs, *EMBO J. 18*, 5120−5130.
25. Zebarjadian, Y., King, T., Fournier, M. J., Clarke, L., and Carbon, J. (1999) Point mutations in yeast CBF5 can abolish in vivo pseudouridylation of rRNA, *Mol. Cell. Biol. 19*, 7461−7472.
26. Perkins, D. N., Pappin, D. J., Creasy, D. M., and Cottrell, J. S. (1999) Probability-based protein identification by searching sequence databases using mass spectrometry data, *Electrophoresis 20*, 3551−3567.
27. Brunger, A. T., Adams, P. D., Clore, G. M., DeLano, W. L., Gros, P., Grosse-Kunstleve, R. W., Jiang, J. S., Kuszewski, J., Nilges, M., Pannu, N. S., Read, R. J., Rice, L. M., Simonson, T., and Warren, G. L. (1998) Crystallography & NMR system: A new software suite for macromolecular structure determination, *Acta Crystallogr., Sect. D: Biol Crystallogr 54*, 905−921.
28. Youssef, O. A., Terns, R. M., and Terns, M. P. (2007) Dynamic interactions within sub-complexes of the H/ACA pseudouridylation guide RNP, *Nucleic Acids Res. 35*, 6196−6206.

BI701606M